International Journal of
Chemical Separation Technology

ISSN: 2456-6691
Volume 12, Issue 1, 2026
January—June
DOI (Journal): 10.37628/IJCST

https://journalspub.com/journal/ijcst/

Research IJCST

Low-Cost FDM-Printed Microfluidic Droplet Generators with Vertical Flow-Focusing Channels

D. M. C. T. Dissanayake[1], L. C. Menikarachchi[2], K. B. Wijayaratne[3], B. S. Nanayakkara[4], L. K. Narangammana[3,*]

Abstract

Low-cost fabrication methods are now essential for expanding access to microfluidic technologies in biological and laboratory applications. In this work, we present a fused deposition modeling (FDM) based approach for the rapid fabrication of monolithic microfluidic droplet generators incorporating several T-junction and specific flow-focusing geometries, including a novel vertical channel configuration. All devices were fabricated without post-processing or bonding, demonstrating a simple and cost-effective workflow using commercially available desktop 3D printers. The fabrication quality and dimensional fidelity of the printed devices were systematically evaluated by comparing channel orientation and printer resolution. Vertical channel architecture exhibited improved channel continuity and reduced blockage compared to conventional horizontal designs. Droplet generation experiments using water-in-oil emulsions revealed stable and reproducible droplet formation across a range of flow conditions. Flow-focusing devices with vertical channels produced smaller droplets with reduced size variability and shorter formation times relative to horizontal configurations. Higher printer resolution further enhanced droplet uniformity and controllability. Finally, the capability of the developed devices for biological applications was demonstrated through the encapsulation of bacterial cells within discrete droplets. The results highlight the potential of low-cost FDM-printed microfluidic devices as accessible platforms for droplet-based biological experiments, particularly in resource-limited research environments.

Keywords: Bacterial cell encapsulation, flow-focusing geometry, fused deposition modeling, microfluidic droplet generators, three-dimensional printing, vertical microchannel architecture

INTRODUCTION

Droplet-based microfluidics has certainly emerged as a powerful platform for applications ranging from chemical synthesis and materials fabrication to biological analysis and diagnostics. By compartmentalizing fluids into discrete, highly uniform droplets, microfluidic systems enable precise control over reaction conditions, reduced reagent consumption, and high-throughput processing. In biological applications, such as cell encapsulation, enzyme assays, and microbial studies, the ability to generate monodisperse droplets with controllable size and formation frequency is particularly critical for ensuring reproducibility and quantitative reliability [1–3].

Traditionally, microfluidic droplet generators have been fabricated using photolithography and soft lithography techniques, commonly employing polydimethylsiloxane (PDMS). While these methods provide excellent spatial resolution and surface quality, they require cleanroom facilities, specialized equipment, and skilled personnel, which significantly increase fabrication cost and limit accessibility,

***Author for Correspondence**
L. K. Narangammana
E-mail: lahirukn@sci.pdn.ac.lk

[1]Research Assistant, Department of Physics, University of Peradeniya, Sri Lanka
[2]Senior Lecturer, Department of Pharmacy, University of Peradeniya, Sri Lanka
[3]Senior Lecturer, Department of Physics, University of Peradeniya, Sri Lanka
[4]Senior Lecturer, Department of Botany, University of Peradeniya, Sri Lanka

Received Date: February 13, 2026
Accepted Date: February 17, 2026
Published Date: March 22, 2026

Citation: D. M. C. T. Dissanayake, L. C. Menikarachchi, K. B. Wijayaratne, L. K. Narangammana, B. S. Nanayakkara. Low-Cost FDM-Printed Microfluidic Droplet Generators with Vertical Flow-Focusing Channels. International Journal of Chemical Separation Technology. 2026; 12(1): 30–46p.

especially in resource-constrained environments [4, 5]. Moreover, planar fabrication methods often restrict device geometries to quasi-two-dimensional designs, limiting the exploration of fully three-dimensional (3D) flow configurations that can enhance droplet control and throughput.

Additive manufacturing, commonly known as 3D printing, has recently emerged as a promising alternative for microfluidic device fabrication. By enabling rapid prototyping, design flexibility, and low-cost production, 3D printing offers a pathway toward democratizing microfluidic technologies [6–8]. Among the available 3D printing techniques, stereolithography (SLA) and fused deposition modeling (FDM) have attracted most attention for microfluidic applications. SLA provides high spatial resolution and smooth surface finishes but relies on expensive, chemically restrictive resins and requires extensive post-processing [9]. In contrast, FDM utilizes thermoplastic materials, such as polylactic acid (PLA), which are inexpensive, chemically resistant, mechanically robust, and widely available, making FDM particularly attractive for low-cost and scalable microfluidic fabrication [10, 11].

Despite its advantages, FDM-based microfluidics faces several challenges, including limited printing resolution, surface roughness, channel deformation, and partial blockage of microscale features. These limitations have historically constrained FDM devices to millifluidic regimes rather than true microfluidic operation [12]. However, recent advances in printer hardware, slicing algorithms, nozzle design, and fabrication strategies have demonstrated that even low-cost desktop FDM printers can reliably produce functional microfluidic devices capable of generating water-in-oil droplets with controlled size and frequency [13–15]. These developments highlight the potential of FDM as a viable fabrication route for droplet-based microfluidics when appropriate design strategies are employed.

Droplet generation in microfluidic systems is commonly achieved using passive geometries such as T-junctions, co-flow, and flow-focusing configurations. Among these, flow-focusing geometries are particularly effective for producing small, monodisperse droplets due to the strong hydrodynamic focusing and shear forces exerted by the continuous phase at the constriction region [16–18]. Conventional flow-focusing devices are typically fabricated in planar geometries, where all channels lie in a single horizontal plane. While such designs are effective, fully three-dimensional flow-focusing configurations can offer additional advantages, including improved symmetry, reduced wetting of channel walls, and enhanced droplet uniformity [19]. However, the fabrication of true 3D flow-focusing geometries has traditionally required complex microfabrication processes, limiting their widespread adoption.

FDM-based 3D printing provides a unique opportunity to explore fully three-dimensional microfluidic geometries without the need for multilayer alignment or bonding. In particular, vertical channel architecture enables the realization of 3D flow-focusing junctions that are difficult to fabricate using conventional planar techniques. Despite this potential, systematic experimental studies investigating droplet generation in FDM-printed flow-focusing devices with vertical channel configurations remain limited. Furthermore, the influence of printer resolution, printing orientation, and channel geometry on droplet size and formation dynamics has not been thoroughly explored in low-cost FDM systems [20–23].

In this work, we report the design, fabrication, and experimental characterization of low-cost FDM-based microfluidic droplet generators incorporating novel flow-focusing geometry with vertical channels. Devices were designed using computer-aided design (CAD) software and fabricated using two commercially available desktop FDM printers with different resolution capabilities. For comparison, both conventional T-junction and flow-focusing geometries were investigated, along with horizontal and vertical channel configurations. Water-in-oil droplets were generated using paraffin oil as the continuous phase and water as the dispersed phase, and droplet size, uniformity, and formation time were systematically analyzed as functions of flow rate and device geometry [24–29].

The results demonstrate that FDM-printed flow-focusing devices with vertical channels can reliably generate monodisperse droplets with tunable diameters and formation frequencies, despite the inherent resolution limitations of FDM printing. The influence of channel orientation and printer resolution on

droplet characteristics is quantified, and the advantages of vertical flow-focusing geometries over conventional planar designs are discussed. Finally, the potential of these low-cost microfluidic droplet generators for biological applications, including microbial encapsulation, is highlighted [30–32].

MATERIALSAND METHODS

Design of Microfluidic Droplet Generators

Microfluidic droplet generators incorporating both T-junction and flow-focusing geometries were designed using computer-aided design (CAD) software (Autodesk Fusion 360). Particular emphasis was placed on developing a three-dimensional flow-focusing geometry with vertically oriented channels, which cannot be easily fabricated using conventional planar microfabrication techniques. All designs employed a nominal channel width of 800 µm and a channel height of 1 mm to ensure reliable device printability using fused deposition modeling (FDM) while maintaining stable droplet generation.

Two design strategies were implemented for flow-focusing devices with horizontal channels, a shelling-based approach and a subtraction-based approach. For vertical channel designs, material was selectively removed along the vertical axis to form a fully three-dimensional flow-focusing junction with aligned inlet and outlet channels in Figure 1.

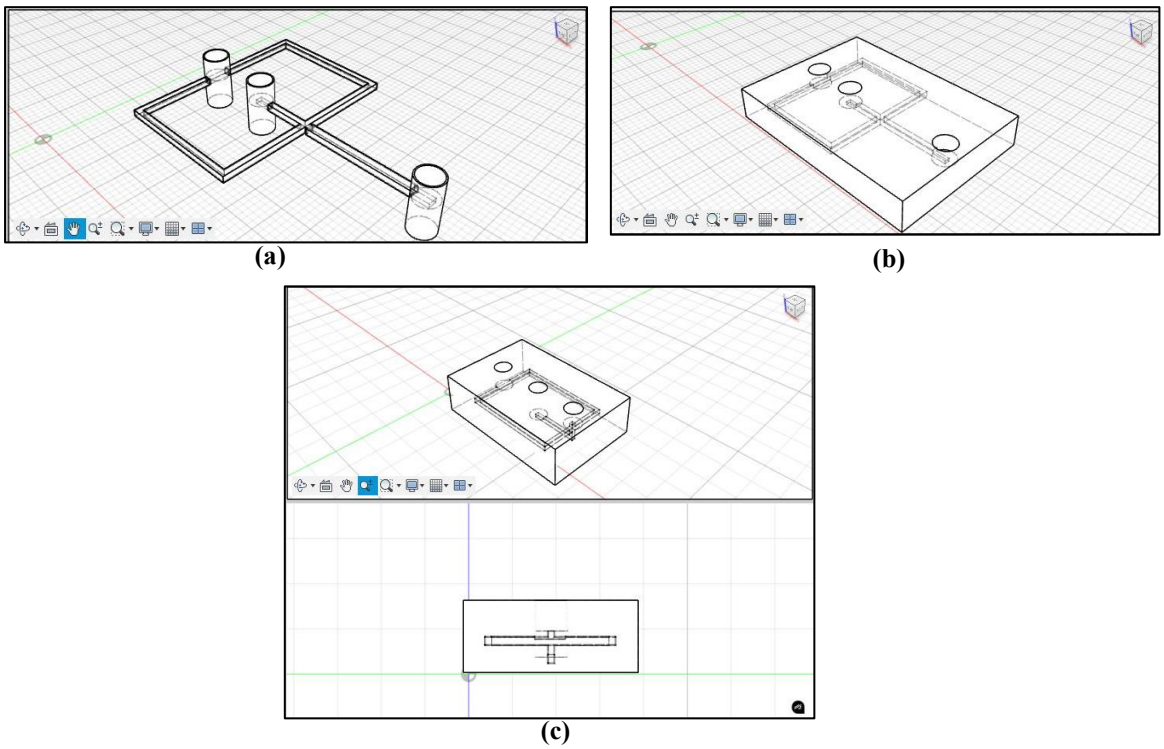

Figure 1. (a) Horizontal channels fabricated using a shelling technique, (b) horizontal channels fabricated using a subtraction approach, and (c) vertical channel flow focusing geometry.

Fabrication Using FDM 3D Printing

The designed microfluidic devices were fabricated using two commercially available desktop FDM 3D printers to assess the influence of printer resolution and material properties on device performance. An Ender printer was operated with a nominal resolution of 100 µm using transparent polylactic acid (PLA) filament to enhance optical visibility during droplet generation. An Ultimaker 2 printer was operated with a nominal resolution of 60 µm using standard PLA filament to improve dimensional accuracy.

All devices were printed as monolithic structures without bonding or post-processing. Printing orientation and slicing parameters were kept constant for each printer to ensure reproducibility across devices.

Experimental Setup for Droplet Generation

Droplet generation experiments were performed using a syringe pump driven flow system. Two independent syringe pumps were used to control the flow rates of the dispersed and continuous phases. Silicone tubing with an inner diameter of 1 mm was used to connect the pumps to the device inlets, while adaptor tubing ensured leak-free connections between components.

Generated droplets were collected at the device outlet in small plastic sample holders to minimize wetting effects and preserve droplet integrity during observation.

Fluids Used and Flow Conditions

Water-in-oil droplets were generated using distilled water as the dispersed phase and paraffin oil as the continuous phase. The dispersed phase was dyed using food coloring and methylene blue to enhance optical contrast during visualization.

The continuous phase flow rate was fixed at 10 mL/h and 20 mL/h, while the dispersed phase flow rate was systematically varied. For devices with vertical channels, the dispersed phase flow rate ranged from 0.2 mL/h to 2.2 mL/h in increments of 0.4 mL/h. For horizontal channel devices, the dispersed phase flow rate ranged from 0.5 mL/h to 3.0 mL/h in increments of 0.5 mL/h.

Droplet Size Measurement

Droplet diameters were measured using optical microscopy. Individual droplets were collected from the outlet region and transferred to sample holders for imaging. For each experimental condition, multiple droplets were measured to evaluate size uniformity and reproducibility. Droplet diameters were extracted from calibrated images using imaging software in Figure 2.

(a) (b)

Figure 2. Optical microscope setup for droplet size measurement. (a) Zeiss Axio Scope ST emi 508 microscopes paired with an Axio Cam digital camera, (b) microscope with monitor.

Droplet Formation Time and Frequency Analysis

Droplet formation dynamics were analyzed using high-resolution video recordings captured at 30 frames per second. The droplet generation region was recorded continuously, and the time required to generate a fixed number of droplets was measured frame by frame. Droplet formation time and generation frequency were calculated from these recordings.

RESULTS

Fabrication Quality and Dimensional Fidelity of FDM-Printed Devices

Microfluidic droplet generators incorporating T-junction and flow-focusing geometries were successfully fabricated using fused deposition modeling (FDM). Representative photographs of the printed devices, including both horizontal and vertical channel configurations, are shown below in Figure 3.

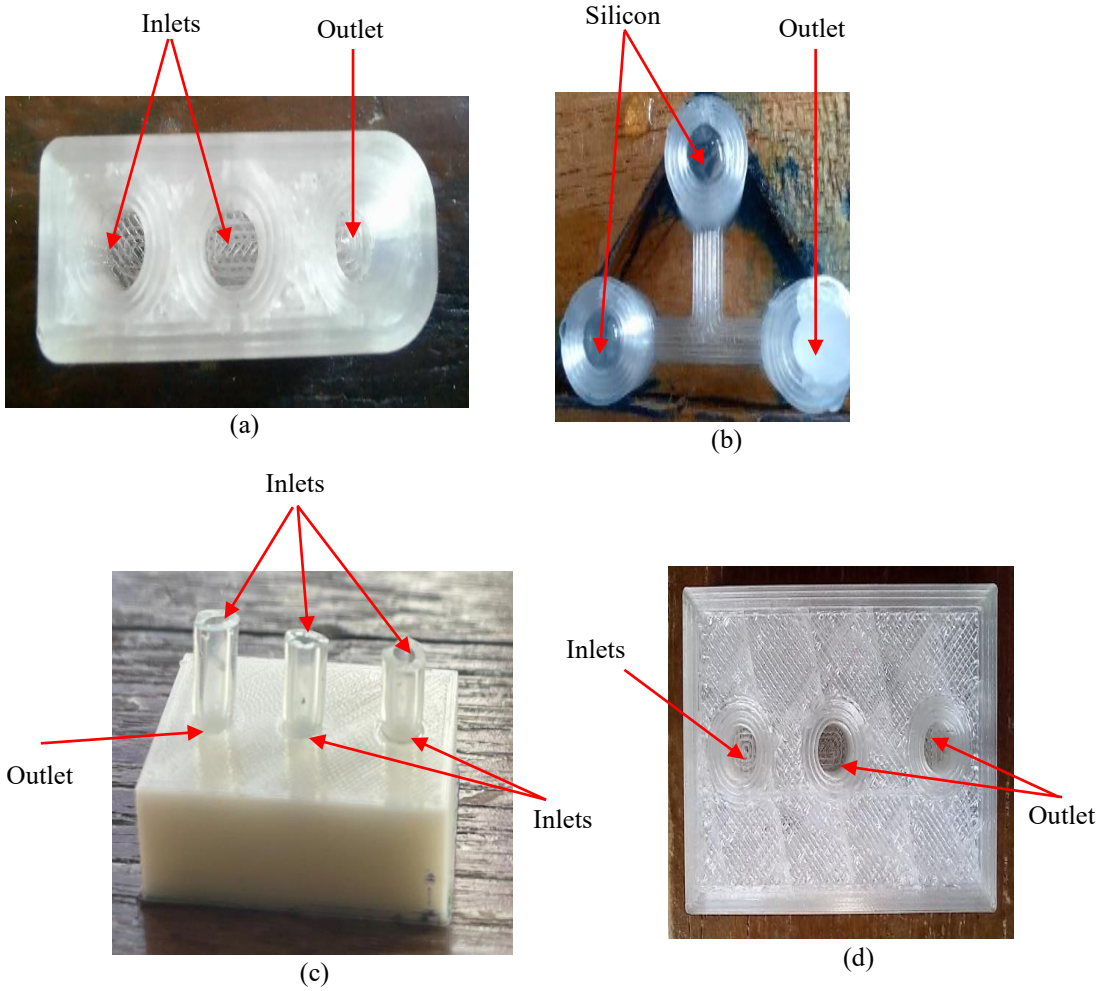

Figure 3. Photographs of FDM printed microfluidic devices (a) T junction geometry device with vertical channels, (b) T junction geometry device with horizontal channels (b) flow focusing device with horizontal channels, and (c) flow focusing device with vertical channels.

All devices were printed as monolithic structures without post-processing or bonding, demonstrating the feasibility of rapid, low-cost fabrication using desktop FDM printers.

Microscopic inspection revealed that fabrication quality depended strongly on both printer resolution and channel orientation. Optical micrographs of printed channels are presented below.

Devices printed using the Ultimaker 2 exhibited smoother channel walls and improved dimensional consistency compared to those printed using the Ender printer. In both printers, vertical channels showed fewer obstructions and more consistent cross sections than horizontal channels, which were more susceptible to partial blockage due to layer-by-layer deposition effects in Figure 4.

Although the nominal design width was 800 µm, the measured widths were significantly smaller, reflecting shrinkage and resolution limitations inherent to FDM printing. These deviations highlight the importance of printer selection and channel orientation in achieving functional microfluidic devices.

Droplet Generation in T-Junction Geometry

To establish a baseline for droplet generation, water-in-oil droplets were produced using an FDM-printed T-junction device with vertical channels. Representative optical images of droplets generated at different dispersed-phase flow rates are shown below in Figure 5.

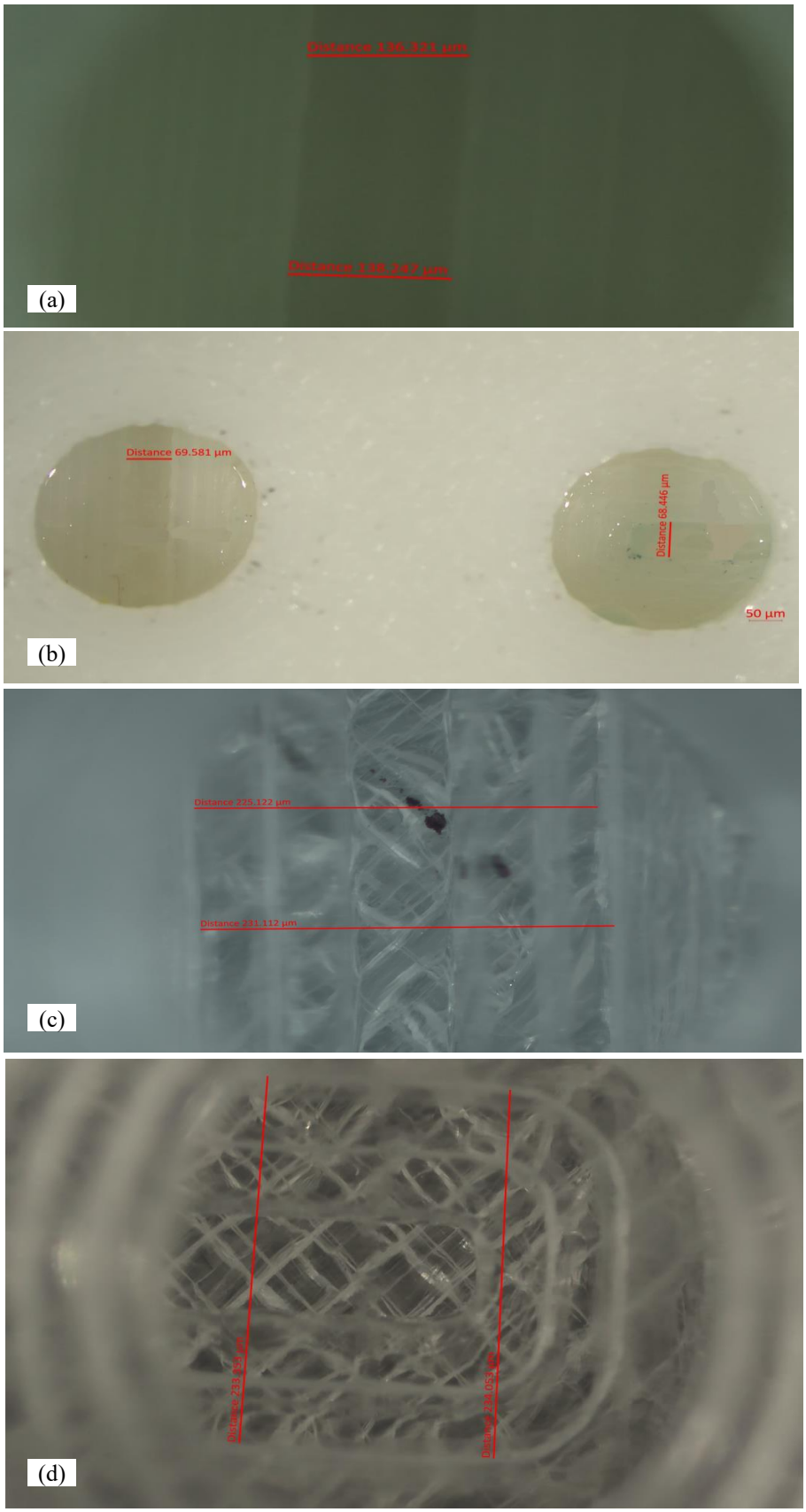

Figure 4. Optical micrographs of printed microchannels: (a) Ultimaker 2 vertical channels, (b) Ultimaker 2 horizontal channels, (c) Ender vertical channels, and (d) Ender horizontal channels.

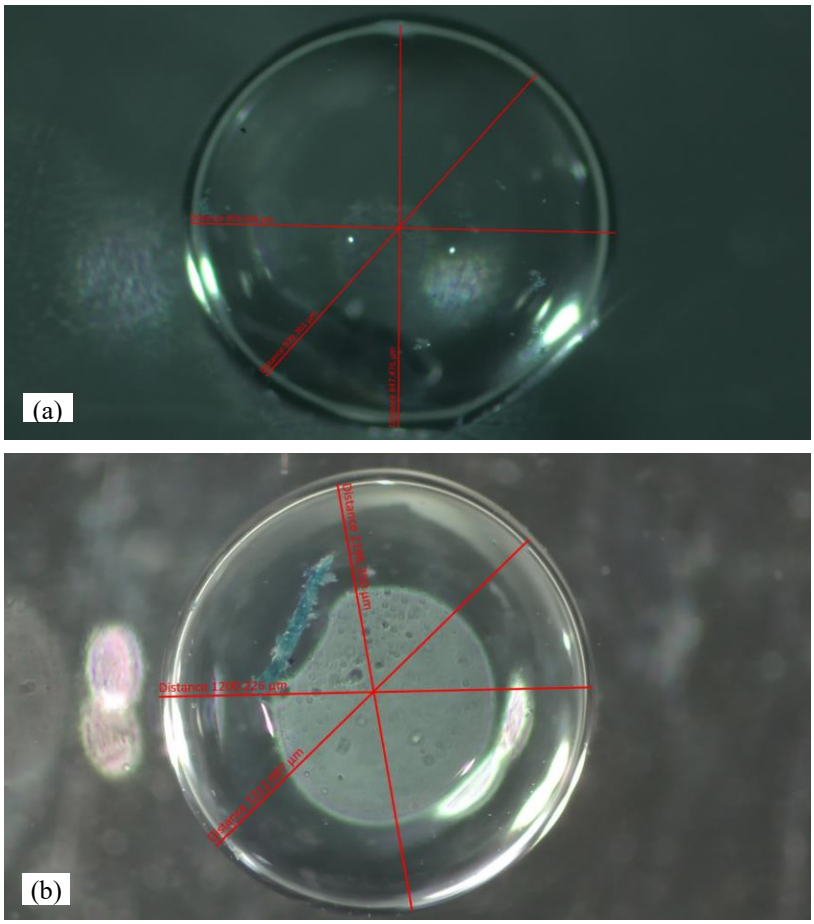

Figure 5. Optical images of droplets generated using a T-junction device at (a) low dispersed-phase flow rated and (b) high dispersed-phase flow rate.

At lower dispersed phase flow rates, larger droplets were observed, while increasing the flow rate led to reduced droplet size. The quantitative relationship between droplet diameter and dispersed phase flow rate is shown below in Figure 6.

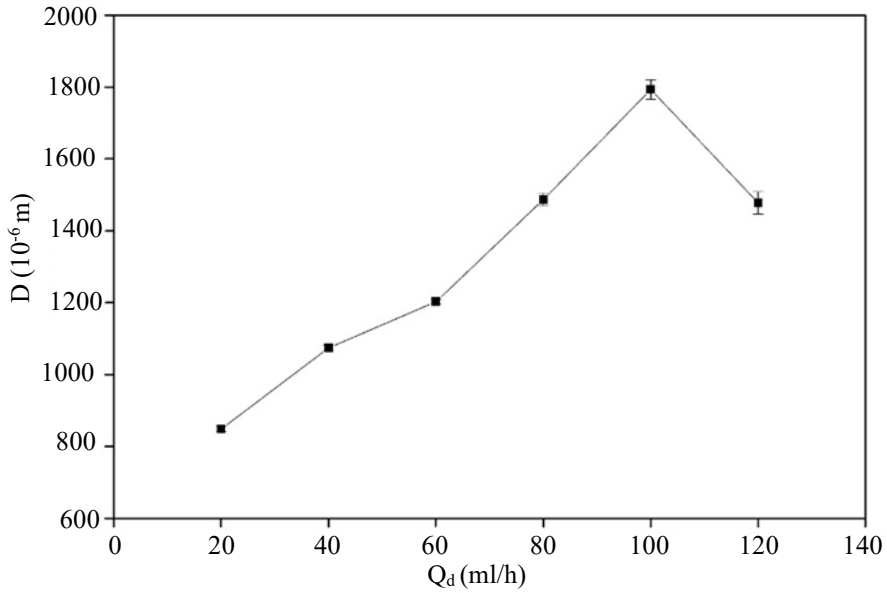

Figure 6. Variation of droplet diameter with dispersed phase flow rate for the T junction geometry.

Corresponding droplet diameter measurements are provided in tabulated form in Table 1.

Table 1. Droplet diameters generated by the T-junction device at different dispersed-phase flow rates.

Flow rate of dispersed phase (Q_d) (ml/h)	Diameter 1 ($\times 10^{-6}$m)	Diameter 2 ($\times 10^{-6}$m)	Diameter 3 ($\times 10^{-6}$m)	Average diameter (D) ($\times 10^{-6}$m)	Standard error (σ) ($\times 10^{-6}$m)
20	859.068	839.361	847.476	848.635	8.087
40	1063.367	1078.435	1081.568	1074.457	7.945
60	1196.350	1200.226	1212.097	1202.891	6.699
80	1463.300	1490.900	1506.600	1486.933	17.898
100	1794.519	1759.591	1825.790	1793.300	27.039
120	1513.602	1438.150	1481.349	1477.700	30.911

While stable droplet formation was achieved, the range of controllable droplet sizes and uniformity was limited compared to flow-focusing geometries, motivating further investigation in Figure 7.

Droplet Generation in Flow-Focusing Devices

Effect of Channel Orientation

Flow-focusing devices with vertical channel configuration were evaluated to investigate the influence of channel orientation on droplet formation. Representative droplet images generated using Ender printed devices are shown below.

Devices with vertical channels consistently produced more uniform and well-defined droplets than horizontal channel devices under comparable flow conditions.

The dependence of droplet diameter on dispersed phase flow rate for Ender printed flow-focusing devices with vertical channels is shown below.

For these configurations, droplet diameter increased with increasing dispersed phase flow rate. However, vertical channel devices produced smaller droplets with reduced size variability. The corresponding numerical data are summarized below in Tables 2 and 3.

Table 2. Droplet diameters with varying dispersed phase flow rate at Q_c = 10 mL/h.

Flow rate of dispersed phase (Q_d) (ml/h)	Diameter 1 ($\times 10^{-6}$m)	Diameter 2 ($\times 10^{-6}$m)	Diameter 3 ($\times 10^{-6}$m)	Average diameter (D) ($\times 10^{-6}$m)	Standard error (σ) ($\times 10^{-6}$m)
0.2	53.62	53.637	54.983	54.080	0.639
0.6	125.052	126.249	126.011	125.771	0.517
1	147.081	147.737	152.497	149.105	2.413
1.4	151.788	155.853	160.882	156.174	3.720
1.8	159.705	160.059	161.738	160.501	0.887
2.2	180.449	181.371	184.048	181.956	1.526

Table 3. Droplet diameters with varying dispersed phase flow rate at Q_c = 20 mL/h.

Flow rate of dispersed phase (Q_d) (ml/h)	Diameter 1 ($\times 10^{-6}$m)	Diameter 2 ($\times 10^{-6}$m)	Diameter 3 ($\times 10^{-6}$m)	Average diameter (D) ($\times 10^{-6}$m)	Standard error (σ) ($\times 10^{-6}$m)
0.2	52.703	53.633	55.268	53.868	1.060
0.6	46.984	47.733	49.116	47.944	0.883
1	41.868	41.894	41.963	41.908	0.040
1.4	57.337	58.413	67.936	61.229	4.763
1.8	97.131	98.787	99.765	98.561	1.087
2.2	134.558	136.446	136.324	135.776	0.863

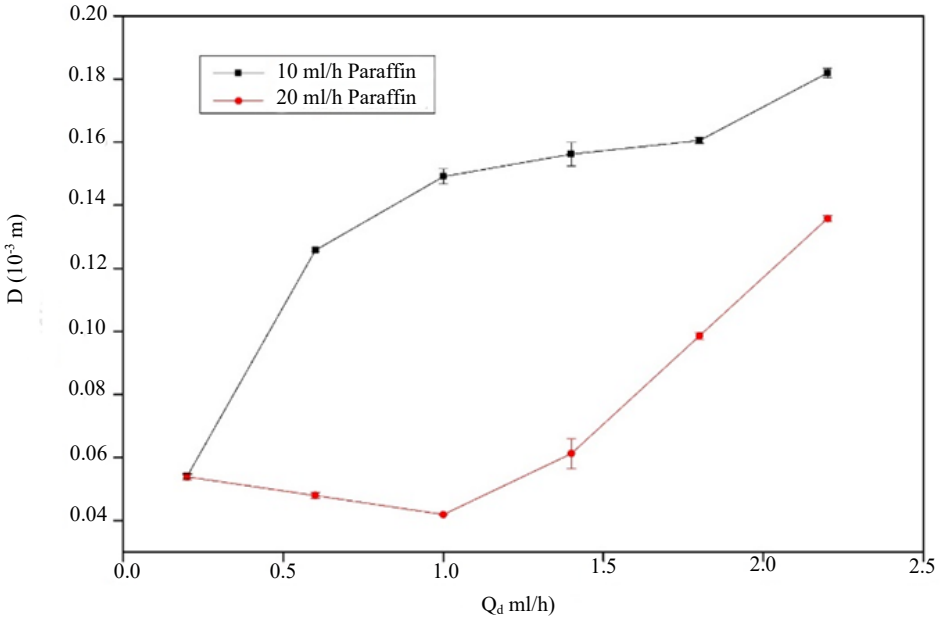

Figure 7. Droplet diameter as a function of dispersed phase flow rate for Ender printed flow focusing devices with vertical channels.

Effect of Printer Resolution

To assess the influence of printer resolution, flow-focusing devices with horizontal channels and vertical channel fabricated using the Ultimaker 2 printer were evaluated. The variation of droplet diameter with dispersed phase flow rate is shown below in Figures 8 and 9.

Compared to Ender printed devices, Ultimaker 2 devices produced smaller droplets with improved.

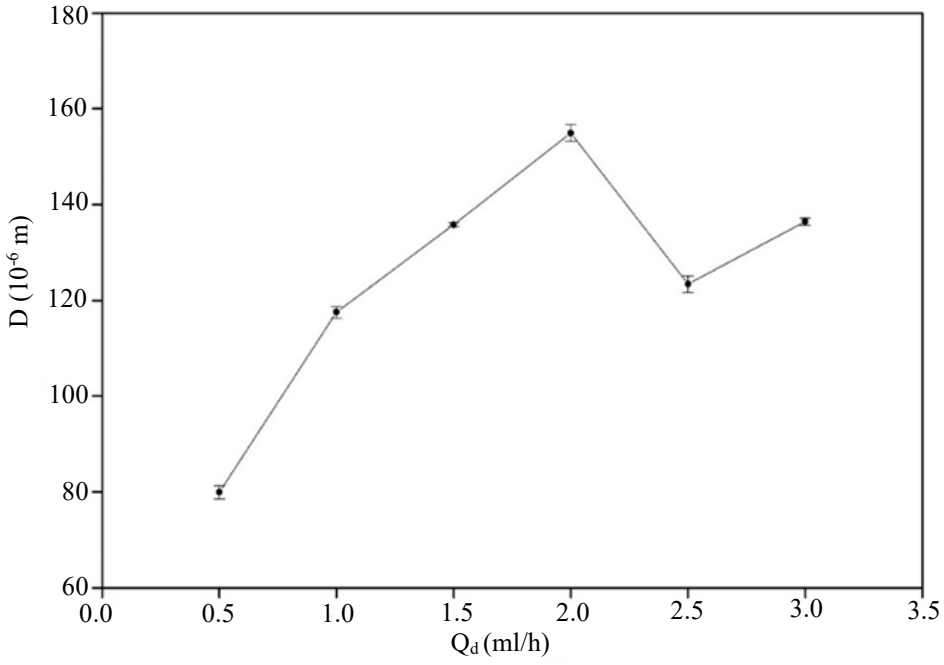

Figure 8. Variation of droplet diameter for the horizontal channel device printed by "Ultimaker 2" for the Q_c = 10 ml/h.

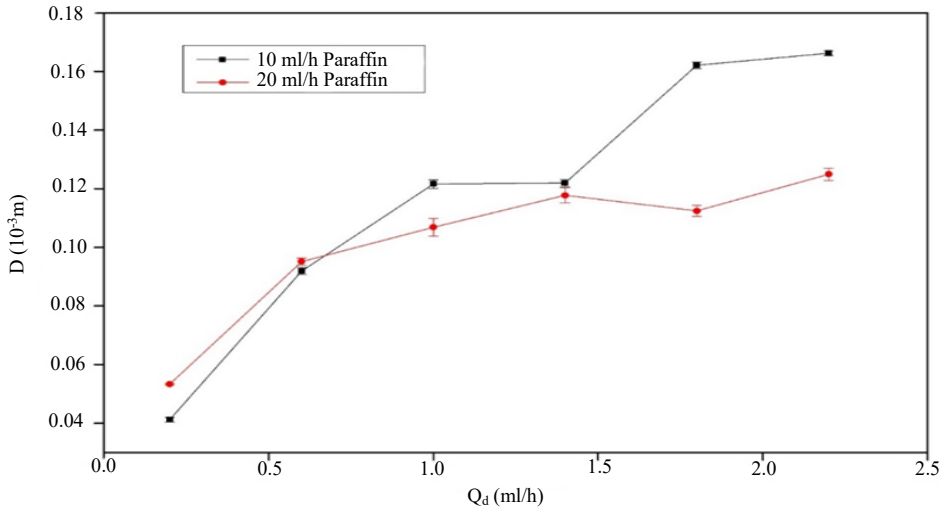

Figure 9. Variation of droplet diameter for the vertical channel device printed by "Ultimaker 2" with the variation of flow rate of the continuous and dispersed phase on droplet size.

Droplet Formation Time and Generation Frequency

Droplet formation dynamics were analyzed using high-resolution video recordings. Sequential frames illustrating the droplet pinch-off process are shown below in Figure 10.

Figure 10. Sequential frames show droplet formation at the flow-focusing junction.

The variation of droplet formation time with dispersed phase flow rate is shown below in Figure 11.

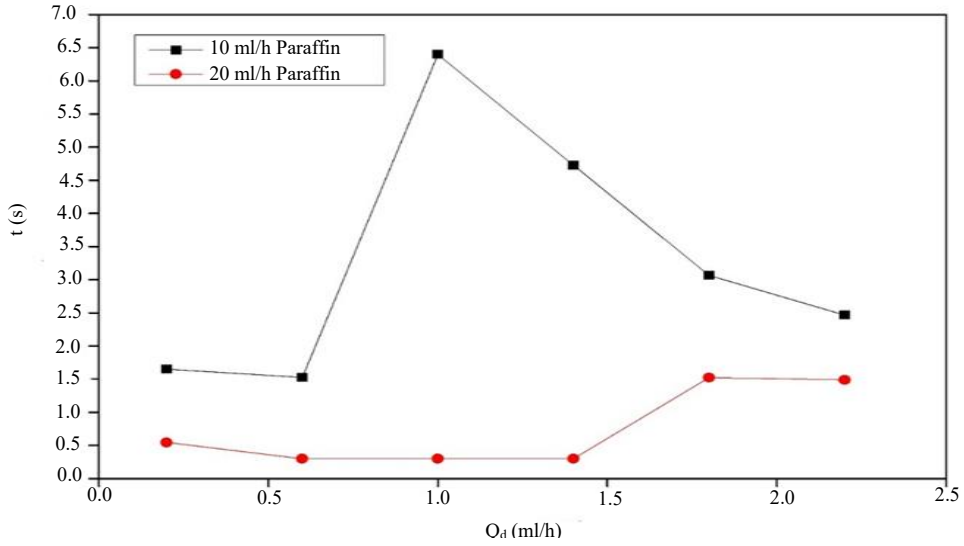

Figure 11. Influence of the flow rate of the continuous and dispersed phase on droplet formation time for the device printed by "Ender" printer with vertical channels in flow focusing geometry.

For all devices, droplet formation time decreased with increasing flow rate, corresponding to higher droplet generation frequencies. Devices with vertical channels consistently exhibited shorter formation times in Figures 12 and 13.

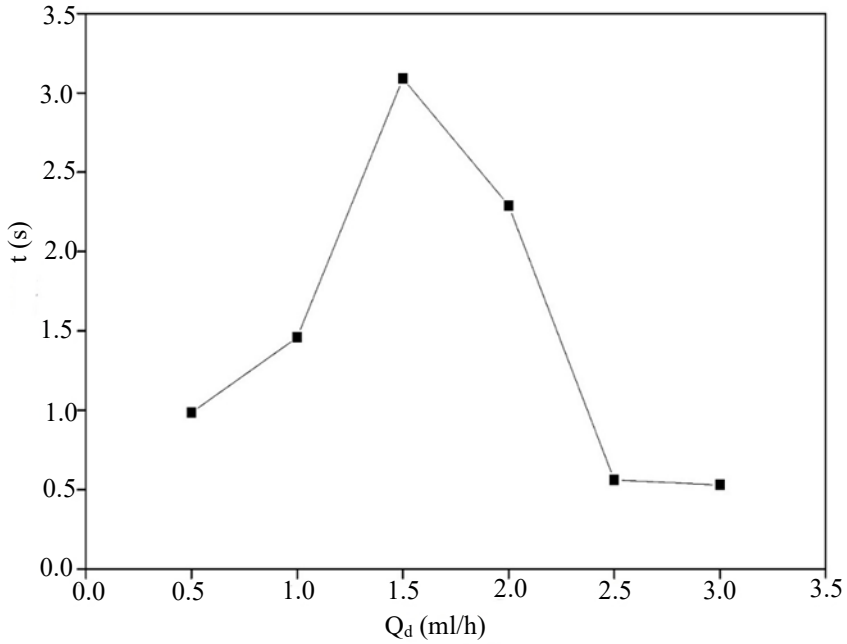

Figure 12. Influence of the flow rate of the continuous and dispersed phase on droplet formation time for the device printed by "Ultimaker 2" printer with horizontal channels in flow focusing geometry.

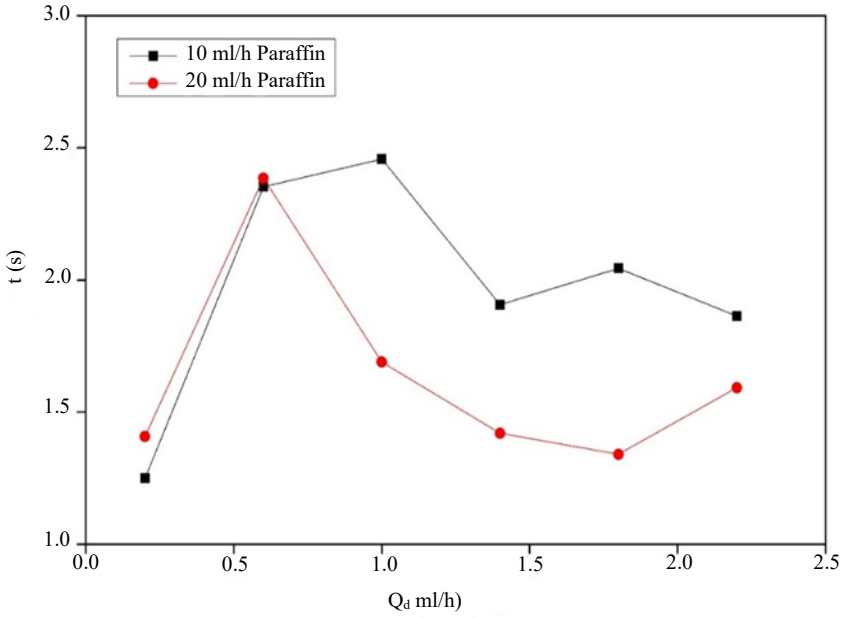

Figure 13. Influence of the flow rate of the continuous and dispersed phase on droplet formation time for the device printed by "Ultimaker 2" with a vertical channel in flow focusing geometry.

Demonstration of Biological Applicability

To demonstrate biological applicability, bacterial suspensions were encapsulated within water-in-oil droplets using optimized flow-focusing devices (device printed by "Ultimaker 2" with a vertical channel).

The device was used for bacterial encapsulation, with the colored bacterial solution as the dispersed phase and paraffin oil as the continuous phase. Qc was set to 20 mL/h and Qd was set to 2 mL/h according to the obtained data. Optical micrographs of bacterial cultures and encapsulated cells are shown below in Figures 14–16.

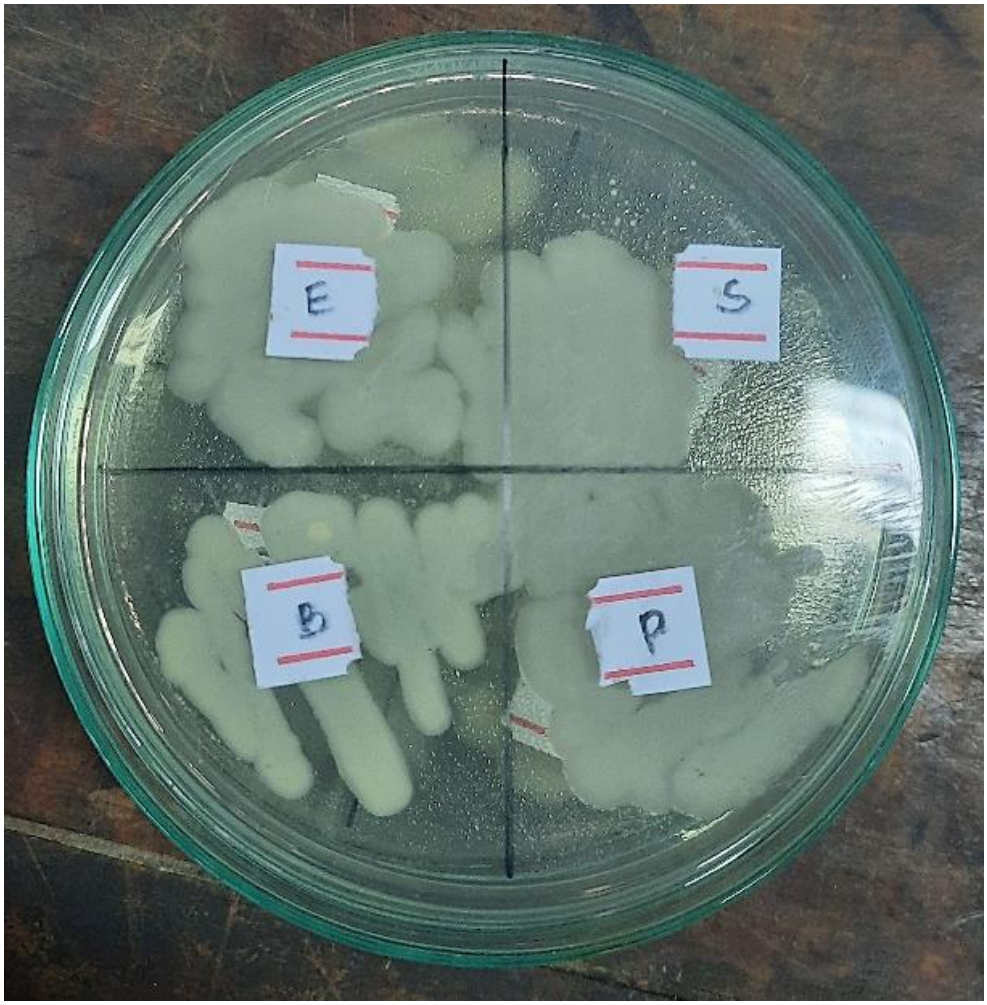

Figure 14. Bacteria cultured in the medium acquired from the department of botany.

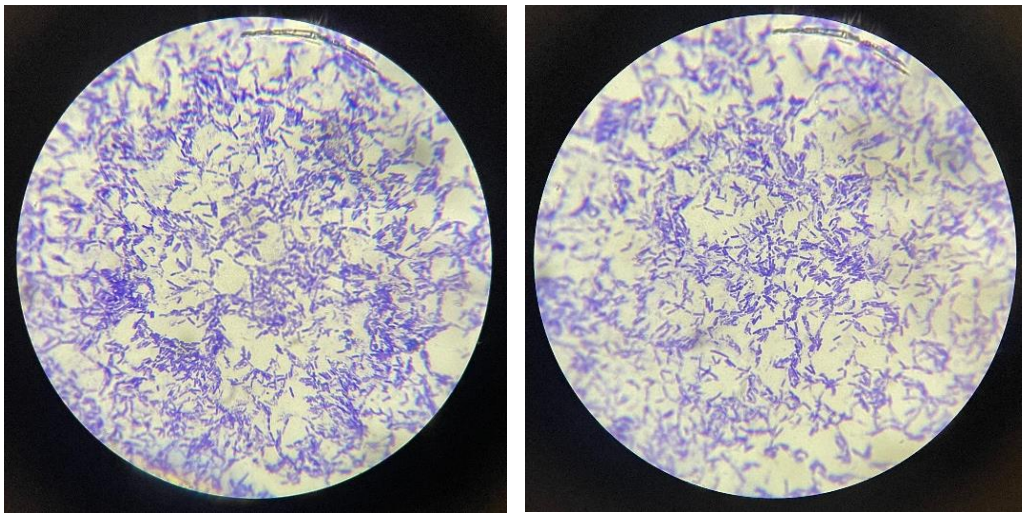

Figure 15. Microscopic images of bacteria used to get an initial bacterial density.

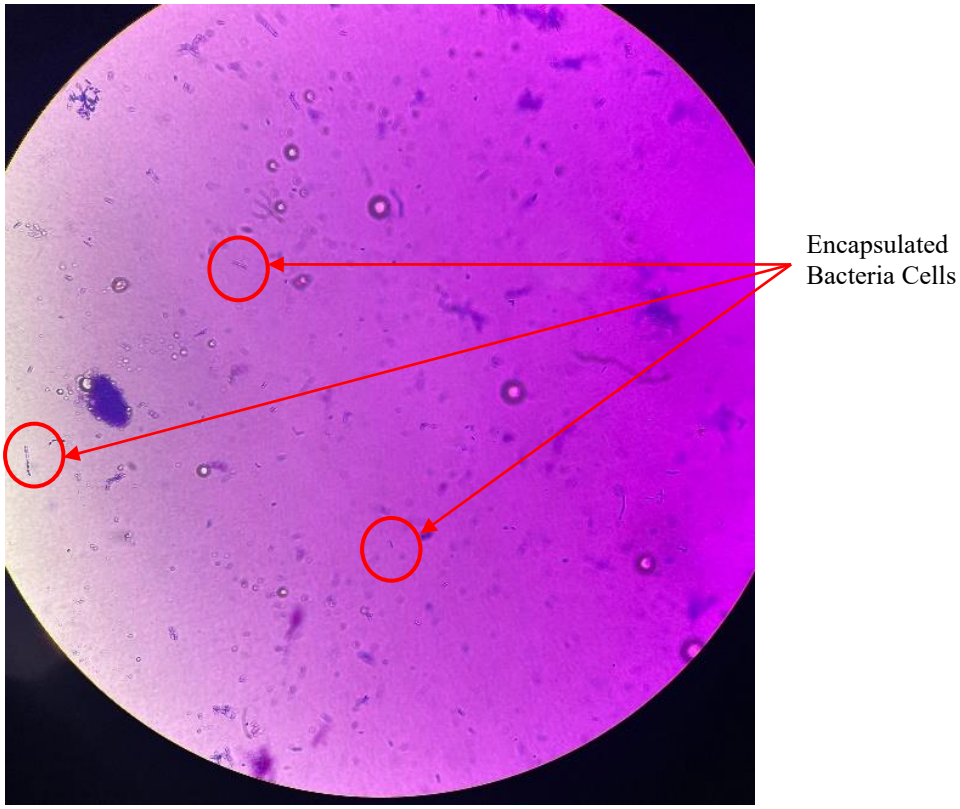

Figure 16. Microscopic image of encapsulated bacteria cells.

Individual bacteria were successfully confined within discrete droplets, confirming the suitability of the developed low-cost microfluidic devices for biological applications.

DISCUSSION

The results presented in this study demonstrate that low-cost fused deposition modeling (FDM) can be successfully employed to fabricate functional microfluidic droplet generators capable of producing water-in-oil droplets with controllable size and generation frequency. Despite the known limitations of FDM printing, including reduced resolution and surface roughness, the fabricated devices consistently enabled stable droplet formation across a range of flow conditions.

Fabrication Quality and Channel Fidelity

The fabrication results confirm that both printer resolution and channel orientation significantly influence the dimensional fidelity of FDM-printed microfluidic channels. As shown by optical micrographs and channel width measurements, devices printed using the Ultimaker 2 exhibited smoother channel walls and more consistent channel dimensions than those printed using the Ender printer. This improvement is reflected in the reduced variability observed in droplet size for Ultimaker 2 devices.

Across both printers, vertical channel configurations exhibited fewer partial blockages and more uniform cross sections compared to horizontal channels. This observation is consistent with the layer-by-layer deposition process inherent to FDM printing, where horizontally oriented channels are more susceptible to sagging and material intrusion during fabrication. The improved structural integrity of vertical channels contributed directly to enhanced droplet generation stability observed in later experiments.

Droplet Generation in T-Junction Geometry

The T-junction device served as a baseline configuration for evaluating droplet generation performance. Stable droplet formation was achieved over the investigated range of dispersed phase flow rates, with droplet diameter increasing monotonically as the dispersed phase flow rate increased. This trend reflects the increasing volumetric contribution of the dispersed phase prior to droplet pinch-off.

However, the T-junction geometry exhibited limitations in terms of droplet size uniformity and controllability. The relatively wide range of droplet diameters and the sensitivity to flow rate variations motivated the exploration of flow-focusing geometries, which provide stronger hydrodynamic control at the droplet formation region.

Effect of Channel Orientation on Flow-Focusing Devices

Flow-focusing devices demonstrated improved droplet control compared to the T-junction geometry, particularly when vertical channel configurations were employed. For Ender printed devices, vertical channels consistently produced smaller and more uniform droplets than horizontal channels at comparable flow conditions. This improvement can be attributed to the enhanced confinement and symmetry provided by the vertical flow-focusing geometry, which promotes more stable pinch-off of the dispersed phase.

The reduced variability in droplet diameter observed for vertical channels suggests that this configuration mitigates some of the fabrication induced irregularities associated with FDM printing. Even when printed using a lower resolution printer, vertical channel devices maintain stable droplet generation over a wider operational window.

Influence of Printer Resolution

Printer resolution played a critical role in determining droplet generation performance. Devices fabricated using the Ultimaker 2 printer consistently produced smaller droplets with improved uniformity compared to those printed using the Ender printer. The narrower and more consistent channel dimensions achieved with higher resolution printing resulted in stronger hydrodynamic focusing at the junction region.

Despite the reduced absolute channel dimensions observed in Ultimaker 2 devices, stable droplet formation was maintained across all tested flow conditions. This indicates that improved dimensional consistency can partially compensate for the intrinsic resolution limitations of FDM printing, enabling reliable microfluidic operation without the need for expensive fabrication techniques.

Droplet Formation Time and Generation Frequency

Analysis of droplet formation time revealed a clear dependence on dispersed phase flow rate for all device configurations. Increasing the dispersed phase flow rate resulted in reduced formation time and increased droplet generation frequency. This trend was consistently observed across both printers and channel orientations.

Devices incorporating vertical flow-focusing channels exhibited shorter droplet formation times than horizontal channel devices under equivalent flow conditions. This result indicates that vertical channel configurations not only improve droplet size control but also enhance throughput, making them particularly attractive for applications requiring high droplet production rates.

Biological Applicability

The successful encapsulation of bacterial suspensions within water-in-oil droplets demonstrates the potential applicability of the developed microfluidic devices for biological applications. The confinement of individual bacteria within discrete droplets confirms that the generated droplets provide sufficient stability and isolation for handling biological samples.

This demonstration validates the suitability of low-cost, FDM-printed flow-focusing devices for applications, such as microbial studies and droplet-based biological assays, where accessibility, rapid fabrication, and cost efficiency are critical considerations.

Fluctuations in Droplet Diameter and Generation Frequency

Although stable droplet generation was achieved across all investigated device configurations, fluctuations in droplet diameter and generation frequency were observed under certain flow conditions. These variations are evident in the measured droplet diameter distributions and in the droplet formation time data presented in the Results section, where increased scatter appears at specific dispersed phase flow rates.

One contributing factor to these fluctuations is the dimensional variability inherent to FDM-printed microchannels. As shown by the channel characterization results, printed channel widths deviated from the nominal design dimensions and exhibited non-uniform cross sections, particularly for horizontally oriented channels and for devices fabricated using the lower resolution printer. Such geometric irregularities can locally alter flow resistance and shear conditions at the droplet formation junction, leading to small variations in droplet pinch-off behavior.

Fluctuations were more pronounced at lower and higher dispersed phase flow rates, where the balance between the continuous and dispersed phases becomes more sensitive to small changes in flow conditions. Under these regimes, minor variations in channel geometry or flow stability can result in noticeable differences in droplet breakup timing, leading to increased dispersion in droplet diameter and generation frequency. This behavior is consistent with the observed increase in variability in both droplet size and formation time at specific flow rate combinations.

Additionally, surface roughness associated with the FDM printing process may contribute to unsteady wetting behavior along the channel walls. Variations in surface texture can influence the local interaction between the fluid phases, particularly near the junction region, causing intermittent changes in droplet detachment dynamics. While such effects did not prevent stable droplet generation, they likely contributed to the observed fluctuations in droplet characteristics.

Despite these variations, devices incorporating vertical flow-focusing channels exhibited reduced fluctuation compared to horizontal channel configurations. The improved symmetry and structural integrity of vertical channels resulted in more consistent droplet pinch-off and more uniform generation frequencies. This observation further supports the effectiveness of vertical channel designs in mitigating fabrication induced inconsistencies inherent to low-cost FDM printing.

Overall, the observed fluctuations in droplet diameter and generation frequency highlight the practical limitations of FDM-based microfluidic fabrication while also demonstrating that careful design choices can significantly reduce their impact. Importantly, these variations remained within acceptable limits for stable droplet generation and did not compromise the overall functionality of the devices.

Overall Implications

Overall, the results of this study highlight that careful design choices, particularly channel orientation and printer selection, can significantly enhance the performance of FDM-printed microfluidic droplet generators. The use of vertical flow-focusing geometries enables reliable droplet generation despite fabrication limitations, supporting the feasibility of low-cost microfluidic platforms for both physical and biological applications.

CONCLUSION

This study demonstrates that low-cost fused deposition modeling (FDM) can be effectively used to fabricate functional microfluidic droplet generators capable of producing water-in-oil droplets with controllable size and generation frequency. Microfluidic devices incorporating T-junction and flow-focusing geometries were successfully designed, fabricated, and experimentally evaluated using commercially available desktop FDM printers.

Fabrication results showed that channel orientation and printer resolution play critical roles in determining channel fidelity and overall device performance. Vertical channel configurations exhibited improved structural integrity and reduced obstruction compared to horizontal channels, leading to more stable and reproducible droplet generation. Devices printed using the higher resolution “Ultimaker 2” printer demonstrated improved dimensional consistency and generated smaller, more uniform droplets compared to devices printed using the Ender printer.

Droplet generation experiments confirmed that flow-focusing geometries provide superior control over droplet size and uniformity compared to the T-junction configuration. Vertical flow-focusing devices consistently produced droplets with reduced size variability and shorter formation times across a range of flow conditions. Although fluctuations in droplet diameter and generation frequency were observed at certain flow rates, these variations were primarily associated with fabrication induced channel irregularities and flow sensitivity inherent to FDM printing. Importantly, such fluctuations remained within acceptable limits and did not compromise stable droplet generation.

The successful encapsulation of bacterial suspensions within water-in-oil droplets further demonstrated the applicability of the developed devices for biological applications. The observed droplet stability and effective confinement of bacteria confirm that low-cost FDM-printed microfluidic platforms can be used for handling biological samples without reliance on complex or expensive fabrication methods.

Overall, this work shows that careful design optimization, particularly the use of vertical flow-focusing geometries and appropriate printer selection enables reliable droplet generation using low-cost FDM-based microfluidic devices. These findings highlight the potential of accessible 3D printing technologies as practical and scalable tools for droplet-based microfluidics in both research and biological applications.

REFERENCES

1. Thorsen T, Roberts RW, Arnold FH, Quake SR. Dynamic pattern formation in a vesicle-generating microfluidic device. Phys Rev Lett. 2001 Apr 30;86(18):4163.
2. Song H, Tice JD, Ismagilov RF. A microfluidic system for controlling reaction networks in time. Angew Chem. 2003 Feb 17;115(7):792–6.
3. Xia Y, Rogers JA, Paul KE, Whitesides GM. Unconventional methods for fabricating and patterning nanostructures. Chem Rev. 1999 Jul 14;99(7):1823–48.
4. Qin D, Xia Y, Whitesides GM. Soft lithography for micro- and nanoscale patterning. Nat Protoc. 2010 Mar;5(3):491.
5. Kolesky DB, Truby RL, Gladman AS, Busbee TA, Homan KA, Lewis JA. 3D bioprinting of vascularized, heterogeneous cell-laden tissue constructs. Adv Mater. 2014 May;26(19):3124–30.
6. Tumbleston JR, Shirvanyants D, Ermoshkin N, Janusziewicz R, Johnson AR, Kelly D, et al. Continuous liquid interface production of 3D objects. Science. 2015 Mar 20;347(6228):1349–52.
7. Au AK, Huynh W, Horowitz LF, Folch A. 3D-printed microfluidics. Angew Chem Int Ed. 2016 Mar 14;55(12):3862–81.
8. Song K, Li G, Zu X, Du Z, Liu L, Hu Z. The fabrication and application mechanism of microfluidic systems for high throughput biomedical screening: A review. Micromachines. 2020 Mar 11;11(3):297.
9. Park Y, Franz CK, Ryu H, Luan H, Cotton KY, Kim JU, et al. Three-dimensional, multifunctional neural interfaces for cortical spheroids and engineered assembloids. Sci Adv. 2021 Mar 17;7(12):eabf9153.
10. Mi S, Du Z, Xu Y, Sun W. The crossing and integration between microfluidic technology and 3D printing for organ-on-chips. J Mater Chem B. 2018;6(39):6191–206.
11. Waldbaur A, Rapp H, Länge K, Rapp BE. Let there be chip—Towards rapid prototyping of microfluidic devices: One-step manufacturing processes. Anal Methods. 2011;3(12):2681–716.
12. Au AK, Lee W, Folch A. Mail-order microfluidics: Evaluation of stereolithography for the production of microfluidic devices. Lab Chip. 2014;14(7):1294–301.
13. Ko J, Lee J. Advanced microfluidic systems with temperature modulation for biological applications. Biomicrofluidics. 2025 May 1;19(3).
14. Cubaud T, Mason TG. Formation of miscible fluid microstructures by hydrodynamic focusing in plane geometries. Phys Rev E. 2008 Nov;78(5):056308.
15. Garstecki P, Fuerstman MJ, Stone HA, Whitesides GM. Formation of droplets and bubbles in a microfluidic T-junction—Scaling and mechanism of break-up. Lab Chip. 2006;6(3):437–46.
16. Anna SL, Mayer HC. Microscale tipstreaming in a microfluidic flow focusing device. Phys Fluids. 2006 Dec 1;18(12).
17. Zhu P, Wang L. Passive and active droplet generation with microfluidics: A review. Lab Chip. 2017;17(1):34–75.

18. Shah RK, Shum HC, Rowat AC, Lee D, Agresti JJ, Utada AS, et al. Designer emulsions using microfluidics. Mater Today. 2008 Apr 1;11(4):18–27.
19. Chan EM, Alivisatos AP, Mathies RA. High-temperature microfluidic synthesis of CdSe nanocrystals in nanoliter droplets. J Am Chem Soc. 2005 Oct 12;127(40):13854–61.
20. Glawdel T, Elbuken C, Ren CL. Droplet generation in microfluidics. In: Encyclopedia of Microfluidics and Nanofluidics. 2013. p. 1–2.
21. Rayner M, Trägårdh G, Trägårdh C. The impact of mass transfer and interfacial expansion rate on droplet size in membrane emulsification processes. Colloids Surf A Physicochem Eng Asp. 2005 Sep 15;266(1-3):1–7.
22. Link DR, Grasland-Mongrain E, Duri A, Sarrazin F, Cheng Z, Cristobal G, et al. Electric control of droplets in microfluidic devices. Angew Chem Int Ed. 2006 Apr 10;45(16):2556.
23. Shi Y, Tang GH, Xia HH. Lattice Boltzmann simulation of droplet formation in T-junction and flow focusing devices. Comput Fluids. 2014 Feb 10;90:155–63.
24. Huebner A, Sharma S, Srisa-Art M, Hollfelder F, Edel JB, Demello AJ. Microdroplets: A sea of applications? Lab Chip. 2008;8(8):1244–54.
25. Hanson Shepherd JN, Parker ST, Shepherd RF, Gillette MU, Lewis JA, Nuzzo RG. 3D microperiodic hydrogel scaffolds for robust neuronal cultures. Adv Funct Mater. 2011 Jan 7;21(1):47–54.
26. Therriault D, White SR, Lewis JA. Chaotic mixing in three-dimensional microvascular networks fabricated by direct-write assembly. Nat Mater. 2003 Apr 1;2(4):265–71.
27. Ahn BY, Duoss EB, Motala MJ, Guo X, Park SI, Xiong Y, et al. Omnidirectional printing of flexible, stretchable, and spanning silver microelectrodes. Science. 2009 Mar 20;323(5921):1590–3.
28. Symes MD, Kitson PJ, Yan J, Richmond CJ, Cooper GJ, Bowman RW, et al. Integrated 3D-printed reactionware for chemical synthesis and analysis. Nat Chem. 2012 May;4(5):349–54.
29. Mathieson JS, Rosnes MH, Sans V, Kitson PJ, Cronin L. Continuous parallel ESI-MS analysis of reactions carried out in a bespoke 3D printed device. Beilstein J Nanotechnol. 2013 Apr 29;4(1):285–91.
30. Wijnen B, Hunt EJ, Anzalone GC, Pearce JM. Open-source syringe pump library. PLoS One. 2014 Sep 17;9(9):e107216.
31. Tsuda S, Jaffery H, Doran D, Hezwani M, Robbins PJ, Yoshida M, et al. Customizable 3D printed 'plug and play' millifluidic devices for programmable fluidics. PLoS One. 2015 Nov 11;10(11):e0141640.
32. Britel A, Tomagra G, Aprà P, Varzi V, Sturari S, Amine NH, et al. 3D printing in microfluidics: Experimental optimization of droplet size and generation time through flow focusing, phase, and geometry variation. RSC Adv. 2024;14(11):7770–8.

